

Trehalose Conjugation Enhances Toxicity of Photosensitizers against Mycobacteria

Amit K. Dutta,[†] Eira Choudhary,^{‡,§} Xuan Wang,[†] Monika Záhorszka,^{||} Martin Forbak,^{||} Philipp Lohner,[⊥] Henning J. Jessen,[†] Nisheeth Agarwal,[‡] Jana Korduláková,^{||} and Claudia Jessen-Trefzer^{*,†,⊥}

[†]Institute of Organic Chemistry, Faculty of Chemistry and Pharmacy, University of Freiburg, Albertstraße 21, 79104 Freiburg, Germany

[‡]NCR-Biotech Science Cluster, Translational Health Science and Technology Institute, Gurugram-Faridabad Expressway, third Milestone, Faridabad, 121001 Haryana, India

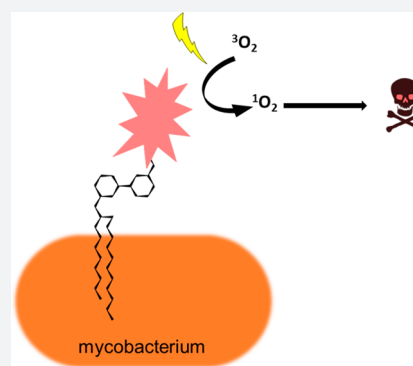
[§]Symbiosis School of Biomedical Sciences, Symbiosis International University, Lavale, Pune, 412115 Maharashtra, India

^{||}Department of Biochemistry, Faculty of Natural Sciences, Comenius University in Bratislava, Mlynská dolina, Ilkovičova 6, 842 15 Bratislava, Slovakia

[⊥]Department of Pharmaceutical Biology and Biotechnology, Faculty of Chemistry and Pharmacy, University of Freiburg, Stefan-Meier-Str. 19, 79104 Freiburg, Germany

S Supporting Information

ABSTRACT: Trehalose is a natural glucose-derived disaccharide found in the cell wall of mycobacteria. It enters the mycobacterial cell through a highly specific trehalose transporter system. Subsequently, trehalose is equipped with mycolic acid species and is incorporated into the cell wall as trehalose monomycolate or dimycolate. Here, we investigate the phototoxicity of several photosensitizer trehalose conjugates and take advantage of the promiscuity of the extracellular Ag85 complex, which catalyzes the attachment of mycolic acids to trehalose and its analogues. We find that processing by Ag85 enriches and tethers photosensitizer trehalose conjugates directly into the mycomembrane. Irradiation of the conjugates triggers singlet oxygen formation, killing mycobacterial cells more efficiently, as compared to photosensitizers without trehalose conjugation. The conjugates are potent antimycobacterial agents that are, *per se*, affected neither by permeability issues nor by detoxification mechanisms via drug efflux. They could serve as interesting scaffolds for photodynamic therapy of mycobacterial infections.



INTRODUCTION

Permeability barriers, off-target binding, upcoming resistance, and the cellular detoxification machinery often lead to early failure in drug development processes.^{1–5} The development of novel antimycobacterial agents, effective against, e.g., *Mycobacterium tuberculosis* (*M. tuberculosis*), the cause of the infectious disease tuberculosis (TB), suffers from the exceptionally restrictive permeability of the cell wall of the *bacilli*. Additionally, active drug export via efflux pumps, upregulated upon the sensing of an unwanted molecule, is potentially reducing drug potency. Strategies to overcome these issues are therefore in high demand and call for the advancement of new assay formats in drug screening and the rational design of molecules to potentially overcome these hurdles. The goal of this study was to develop a potent antimycobacterial agent that is, *per se*, affected neither by permeability issues nor by detoxification mechanisms via drug efflux. Permeability barriers can be overcome by potent toxic compounds that do not act from within the cell and, hence, have no need to pass through the membranes. Likewise, drug efflux is not an issue if the active agent is covalently linked to cellular constituents. In

recent years, several groups have reported on trehalose–fluorophore conjugates or trehalose-derived positron emission tomography (PET) probes. These are useful tools in diagnostics for imaging and detection of live mycobacteria *in vitro*, in human macrophages and in sputum samples from TB patients (Figure 1).^{6–9} The nonmammalian disaccharide trehalose is essential for mycobacteria and is found in the outer portion of the mycobacterial cell envelope as part of the two major glycolipids trehalose dimycolate (TDM) and trehalose monomycolate (TMM).¹⁰ The extracellular Ag85 protein complex catalyzes the reversible transesterification reaction between two units of TMM, generating TDM and free trehalose (Figure 1). Additionally, it catalyzes the transfer of mycolic acids from TMM to arabinose motifs in the cell wall arabinogalactan.¹¹ Ag85 consists of three secreted enzymes Ag85A, Ag85B, and Ag85C. While a deletion of the gene encoding Ag85C does not affect the production of TDM, the silencing of the genes encoding Ag85A and Ag85B leads to a

Received: December 23, 2018

Published: March 27, 2019

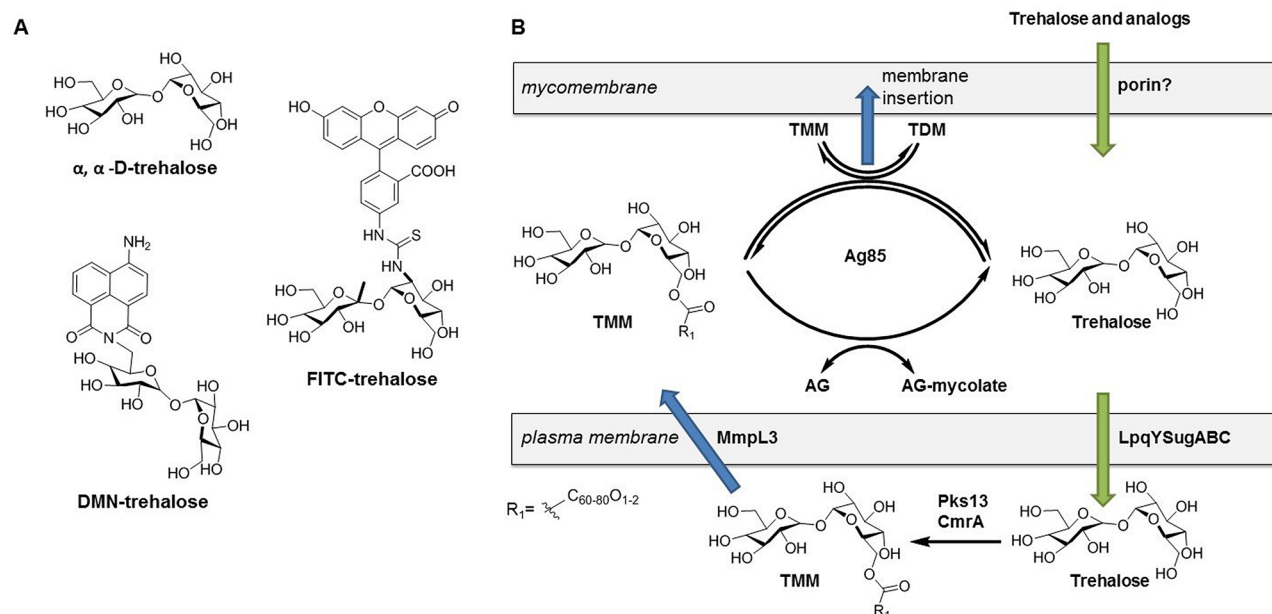


Figure 1. Trehalose and its analogues. (A) Chemical structures of naturally occurring trehalose and published analogues applied in mycobacterial research. (B) Schematic representation of the trehalose uptake/reuptake pathway and its incorporation into the mycomembrane as trehalose dimycolate (TDM) or trehalose monomycolate (TMM).⁷

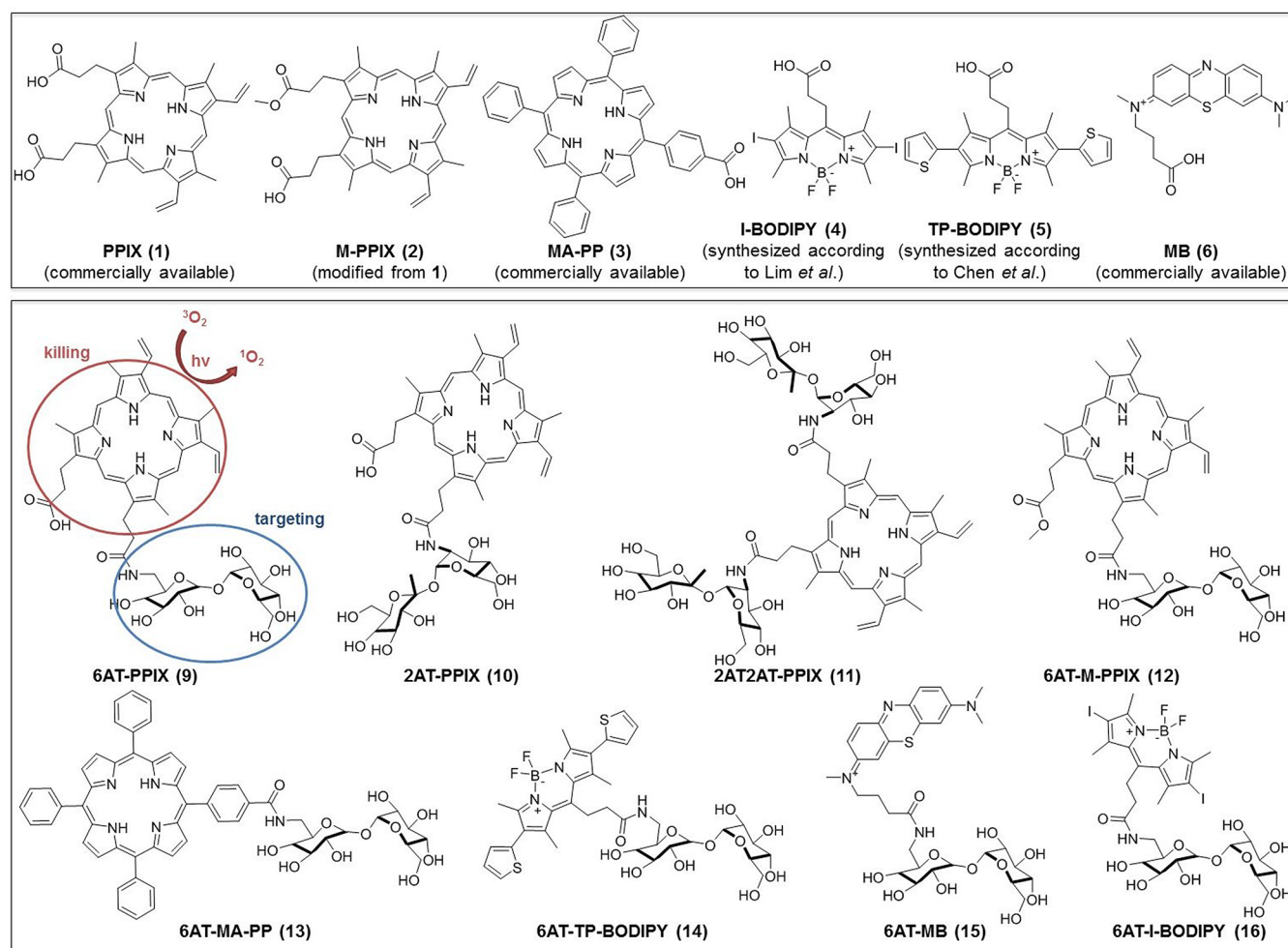


Figure 2. Structures of trehalose-tethered photosensitizers 9–16 and the precursor molecules 1–6. The red circle highlights the toxic warhead of the conjugate and the blue circle the targeting moiety.

Table 1. Minimal Inhibitory Concentrations (μM) of Compounds against *M. smegmatis* and *M. abscessus* and Ability To Generate Singlet Oxygen after Irradiation with a High-Pressure Sodium Light Source^a

	singlet oxygen generation ^b	MIC (μM)			
		<i>M. smegmatis</i> mc ² 155		<i>M. abscessus</i> subsp. abscessus	
		no irradiation	590 nm irradiation	no irradiation	590 nm irradiation
PPIX (1)	0.5	>200	>200	>200	0.26
MA-PP (3)	n.d.	>200	>200	n.d. ^c	n.d.
I-BODIPY (4)	1.1	>200	6.3	>200	4.2
TP-BODIPY (5)	0.1	>200	25	>200	33
MB (6)	1	50	6.3	n.d.	n.d.
6AT (7)	n.d.	>200	>200	n.d.	n.d.
6AT-PPIX (9)	n.d.	>200	>200	n.d.	n.d.
2AT-PPIX (10)	0.6	>200	>200	>200	3.1
2AT2AT-PPIX (11)	1.0	>200	3.1	>200	33
6AT-M-PPIX (12)	n.d.	>200	>200	n.d.	n.d.
6AT-MA-PP (13)	n.d.	>200	>200	n.d.	n.d.
6AT-TP-BODIPY (14)	0.6	50	0.78	>200	0.52
6AT-MB (15)	n.d.	200	25	n.d.	n.d.
6AT-I-BODIPY (16)	1.6	200	1.6	>200	0.78
rifampicin	n.d.	25	25	n.d.	n.d.
SQ109	n.d.	100	100	13	13
ciprofloxacin	n.d.	0.21	0.21	n.d.	n.d.
amikacin	n.d.	0.59	0.59	3.1	3.1

^aMICs were determined by resazurin microtiter assay. Analysis was performed in duplicates and repeated at least in two independent experiments. Visual MIC was defined as the lowest concentration of drug that prevented a color change (blue/resazurin to pink/resorufin). ^bRelative to methylene blue (fluorescence quantification of singlet oxygen sensor green, see main text and the [Supporting Information](#)). ^cn.d.: not determined.

decreased synthesis of this lipid.^{12,13} Interestingly, Ag85 has a large substrate promiscuity, accepting modifications on the trehalose molecule during transesterification reaction. The resulting modified trehalose esters can be subsequently incorporated into the mycobacterial cell wall.^{6–9} Ag85 expression is essential for survival of *M. tuberculosis* within macrophage-like cell line models, and its homologues have been found in a variety of other mycobacterial species such as *Mycobacterium smegmatis* (*M. smegmatis*), *Mycobacterium abscessus* (*M. abscessus*), and *Mycobacterium bovis* (*M. bovis*).⁸ Trehalose mycolates are unique to the phylum Actinobacteria and are completely absent from human metabolism, making Ag85 an attractive drug target. Importantly, it is (I) localized extracellularly and (II) able to utilize modified substrate analogues. In the past, several groups have published reports on the covalent inhibition of Ag85 targeting the catalytic triad in the active site with activity-based probes^{14–17} or a reactive cysteine residue close to the substrate binding pocket.¹⁸

Rather than designing a classical enzyme inhibitor, we decided to use Ag85 for the incorporation of photosensitizers in the form of modified mycobacterial lipids into the mycomembrane. Such molecules are toxic due to the generation of singlet oxygen only during irradiation, which activates the killing agent in a localized and time-dependent fashion. Singlet oxygen release has been reported to be favored in lipid environments such as membranes, which is an additional advantage of this approach.¹⁹ While photodynamic therapy has been proposed previously as an efficient approach to treat multi-drug-resistant TB, there are no study reports on the development of any specific compound to date.^{20–22} As photosensitizer warheads, we investigate porphyrin derivatives, which are well-established in the photodynamic therapy of several cancers, such as lung or skin cancer.²³ Furthermore, we explore the toxicity of BODIPY dyes^{19,24,25} irradiated with a high-pressure sodium lamp and also that of methylene blue,²⁶ a

well-studied photosensitizer for treatment of basal cell carcinoma, Kaposi's sarcoma, melanoma, and viral and fungal infections. Herein, we provide synthetic strategies to obtain several trehalose–photosensitizer conjugates and report their bactericidal activities against mycobacteria.

RESULTS AND DISCUSSION

To explore the potential of photosensitizer trehalose as antibacterial agents, we designed a set of diverse compounds. This strategy enabled the evaluation of the efficacy of several sensitizers 1–6^{24,25} coupled to different modified trehalose analogues (6-amino trehalose (7)²⁷ or 2-amino-7-methyl-trehalose (8),⁶ see the [Supporting Information](#)), following a rapid peptide-coupling protocol. Together, these synthetic routes allowed ready access to several trehalose analogues 9–16 ([Figure 2](#)) for comparison of their toxicity against mycobacteria upon irradiation.

Trehalose conjugates were analyzed regarding their phototoxicity against *M. smegmatis* and *M. abscessus* in a resazurin microtiter assay, and activity was compared to the non-conjugated photosensitizers. *M. smegmatis* is a saprophyte and a well-established model organism in mycobacterial research, while *M. abscessus* is a relevant mammalian pathogen. For phototoxicity assays, cells were grown in 96-well plates and incubated with the compound of interest for 24 h to allow for efficient incorporation of the trehalose-coupled photosensitizers.⁶ Subsequently, the plate was irradiated with a high-pressure sodium lamp (10 mW/cm², 550–650 nm broad emission peak²⁸ to allow efficient activation of the diverse set of compounds). In a prescreening effort, we determined an optimal irradiation time of 15–30 min for efficient killing of *M. smegmatis*, and consequently in the following assays, we irradiated the assay plates for 30 min (see [Figure S1](#) for irradiation time-dependent killing curves). Control plates were

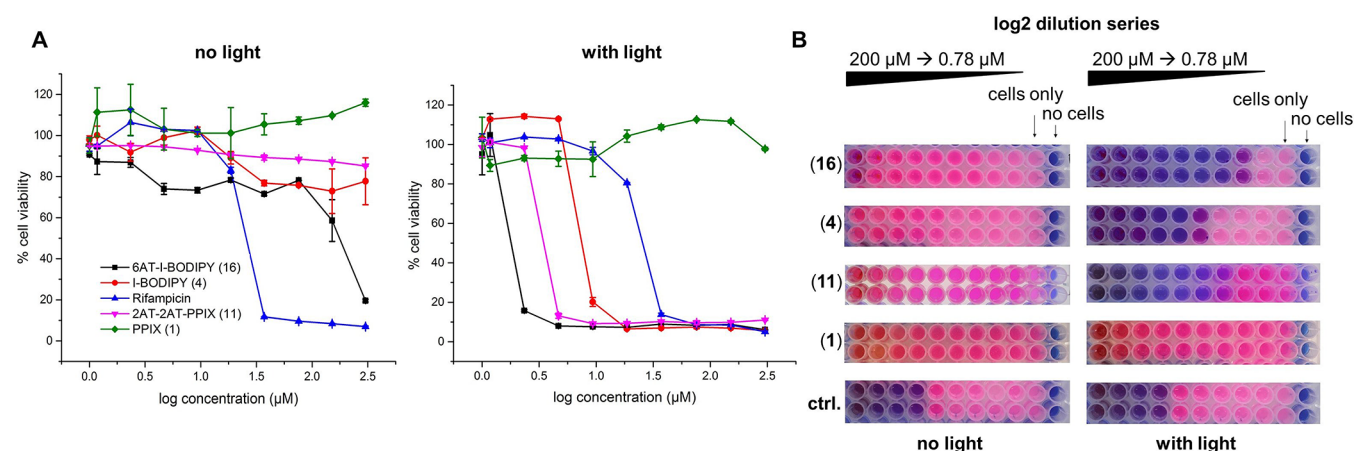


Figure 3. Ability of trehalose-tethered photosensitizers to kill *M. smegmatis* after irradiation with a high-pressure sodium lamp. Free uncoupled photosensitizers I-BODIPY (4) and PPIX (1) show less or no activity against *M. smegmatis*, while the corresponding trehalose-coupled analogues 6AT-I-BODIPY (16) and 2AT2AT-PPIX (11) are potent cytotoxic agents in the presence of light. (A) Cell viability as a function of compound concentration (logarithmic scale), as determined by resazurin-reduction assay. Data obtained from three independent experiments. Error bar indicates \pm SEM. Control compound is rifampicin (blue line). (B) Images of the resazurin-reduction assay in 96-well plate format. Two lanes of wells represent duplicates. Blue indicates cell death or no cells; pink indicates cell survival.

kept in the dark. As positive controls, the anti-TB drugs rifampicin, ciprofloxacin, and amikacin, as well as a drug in clinical development SQ109,²⁹ were used. The measured minimal inhibitory concentrations (MICs) are summarized in Table 1.

Compounds 9, 10, 12, and 13 did not inhibit growth of *M. smegmatis* under the tested conditions, even upon irradiation. However, compounds 11, 14, 15, and 16 showed MICs in a low μ M range after irradiation. Despite 14, 15, and 16 being slightly toxic already without irradiation, they showed a 60-, 8-, and 120-fold increased toxicity upon irradiation, respectively. In contrast 11 was nontoxic in the absence of light even at the highest concentration tested (which is 200 μ M), resulting in an increased toxicity of approximately 2 orders of magnitude upon irradiation (Figure 3 and Table 1). The obtained MIC values of these compounds are comparable with MICs from well-known antimycobacterial agents such as ciprofloxacin or amikacin. While for 11 the corresponding free protoporphyrin IX (1) is nontoxic in both the presence and absence of light, a different behavior is observed for the BODIPY-derived photosensitizers: the unmodified BODIPY derivatives 4 and 5 exhibit increased cytotoxicity against *M. smegmatis* in the presence of light. However, the trehalose conjugates 14 and 16 of these BODIPY derivatives are still significantly more phototoxic (Figure 3 shows representative cell viability data for compounds 4 and 16). Interestingly, methylene blue (6) is already inhibiting growth of *M. smegmatis*, in both the presence and absence of light, at lower concentrations as compared to its trehalose conjugate 15 (Table 1). This observation points toward a different mechanism of action, which deviates from simple incorporation of the compound as a glycolipid into the mycomembrane followed by singlet oxygen generation after irradiation. Indeed, methylene blue is known to penetrate into *tubercle bacilli*, and is often used as a counterstain in histology. Hameed et al. showed that methylene blue causes energy-dependent membrane perturbation and DNA damage in *M. smegmatis*.³⁰ Hence, it is possible that tethering methylene blue to trehalose hinders the compound from entering cells and consequently abolishes additional intracellular toxicity, as described above.

These results provide the first evidence that the attachment of trehalose and its analogues generally has the potential to significantly increase the activity of phototoxic compounds against mycobacteria. Upon comparison of 4/16 and 5/14, the coupling of I-BODIPY (4) or TP-BODIPY (5) to 6-amino-trehalose (7) increases the potency of the resulting conjugates 16 and 14 by 4- and 30-fold. Coupling PPIX (1) to two molecules of 2-amino-7-methyl-trehalose (8) leads to a 60-fold increase in activity of the resulting molecule 11 (Table 1). There are two potential reasons for this behavior: either incorporation of 16, 14, and 11 into the mycomembrane is efficiently taking place, thereby increasing the local concentration of the photosensitizer and consequently also of singlet oxygen, or singlet oxygen generation is influenced by the presence of the trehalose moiety.

To better understand these observations, we investigated the potential of these compounds to generate singlet oxygen upon irradiation. We applied a commercial fluorescence-based assay, in which the probe singlet oxygen sensor green (SOSG)³¹ is incubated with the respective photosensitizers during irradiation. SOSG selectively reacts with singlet oxygen, producing a fluorescent product, which can be quantified following excitation/emission at 504/525 nm (Figure S2). The observed response was overall in agreement with our detected MIC values, and Table 1 shows singlet oxygen release of our most potent compounds and methylene blue (6) as reference. 6AT-I-BODIPY (16) and 2AT2AT-PPIX (11) showed good toxicity against *M. smegmatis* and likewise exhibited the most intense signal in the SOSG assay, while the noncoupled derivative I-BODIPY (4) and PPIX (1) displayed reduced generation of singlet oxygen as compared to their parent compound. Interestingly, 6AT-TP-BODIPY (14) showed only minor singlet oxygen generation, yet significant cytotoxicity, indicating that singlet oxygen release is not the exclusive mechanism of action of this molecule. Importantly, for all compounds tested, we observed a difference in potency when coupled to trehalose. Coupling to trehalose apparently increased singlet oxygen release in the order of PPIX (1) < 2AT-PPIX (10) < 2AT2AT-PPIX (11), indicating that the observed differences in MIC values are a result not only of

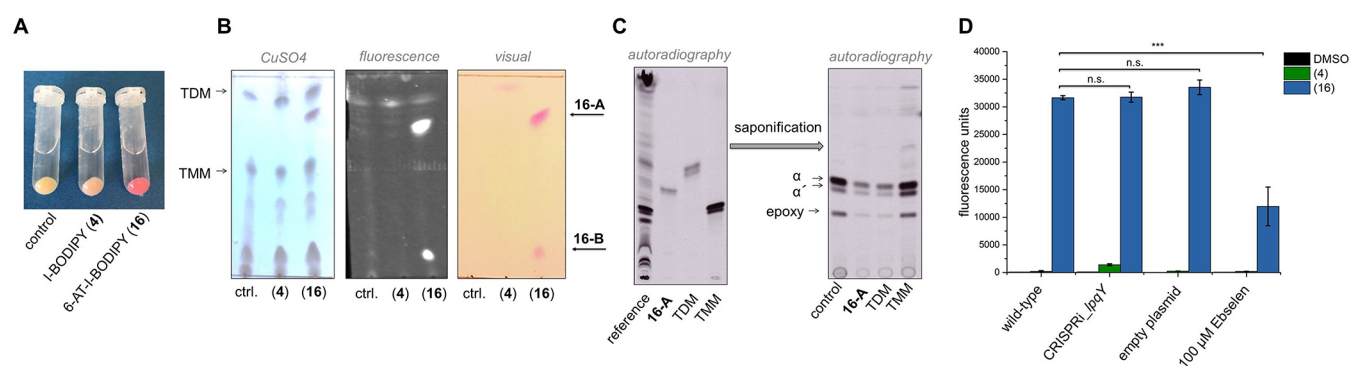


Figure 4. Characterization of the trehalose conjugates. (A) Trehalose-coupled molecule 6AT-I-BODIPY (**16**) incorporates into cells of *M. smegmatis* as indicated by the pink color of the cell pellet. Corresponding uncoupled molecule I-BODIPY (**4**) is not staining the cells. (B) Cells were incubated with the molecules of interest, and after dual washings, cell lipids were extracted with chloroform/methanol. The isolated lipids were resolved by TLC (chloroform/methanol/water 20:4:0.5) and stained with CuSO_4 to visualize lipid species. Visual inspection and fluorescence imaging of the TLC plate revealed two fluorescent species **16-A** and **16-B** after incubation with **16** but not with **4**. Two independent experiments were performed, yielding similar results. (C) Cultures were labeled with ^{14}C acetate in the presence of **16**, and subsequently **16-A**, TMM, and TDM were isolated by preparative TLC (purified isolated fractions are shown, reference is total lipid profile, chloroform/methanol/water 20:4:0.5). Saponification and TLC analysis of corresponding methyl esters revealed that **16-A** consists of MAMEs (solvent: ethyl acetate/hexane 95:5, 3 runs). Two independent experiments were performed, yielding similar results. (D) Incorporation of **16** is not dependent on the trehalose transporter substrate binding protein LpqY but on the acyltransferase Ag85. Pretreatment of *M. smegmatis* with the Ag85 inhibitor Ebselen is lowering incorporation of **16** into lipids to 60%, while silencing of *lpqY* is not significantly abrogating incorporation of **16** into the mycomembrane. Quantification of **16** was done by fluorescence measurement of the isolated lipid extract at $E_{\text{ex}}/E_{\text{em}}$: 525/600 nm. Analysis was done in triplicates; error bars indicate \pm SD. *** Analysis of variance (OriginPro2015), $P < 0.001$; n.s. not significant.

probe incorporation into the mycomembrane but also of the amount of singlet oxygen generated.

Next, a series of experiments were performed to confirm that the compounds are incorporated into the mycomembrane as trehalose mycolates. We focused our experiments on 6AT-I-BODIPY (**16**) and I-BODIPY (**4**), because of the ease of probe detection; we made use of the fluorescence of the attached BODIPY dye. Cultures of *M. smegmatis* were incubated with compounds **16** and **4** for 6 h, and harvested, and the cell pellets were washed twice to remove any nonspecifically bound compound. Importantly, cell pellets of cultures treated with **16** were highly colored, whereas cells treated with DMSO or control compound **4** were noncolored (Figure 4A). These results already pointed toward a successful incorporation of the trehalose conjugate. Subsequently, the lipids were extracted with chloroform/methanol (1:2 and 2:1), washed as described by Folch,³² and resolved by thin-layer chromatography (TLC) in chloroform/methanol/water (20:4:0.5). TLC plates were analyzed visually as well as under fluorescent light and stained with CuSO_4 to visualize lipid species (Figure 4B). Clearly, lipid samples from cells incubated with compound **16** displayed colorful spots with $R_f = 0.65$ (**16-A**) and $R_f = 0.15$ (**16-B**). While migration of **16-B** corresponds to the R_f of compound **16** itself, the appearance of spot **16-A** detectable by fluorescence and CuSO_4 staining indicates processing of compound **16** by mycobacterial enzyme(s). To validate this hypothesis, we performed a similar experiment treating *M. smegmatis* cells with compound **16** in the presence of ^{14}C acetate, a metabolic label, added to the culture 16 h after the tested compound. TLC analysis of extracted lipids revealed the production of a labeled lipid, migrating with the same R_f as **16-A**, in the cells treated with compound **16**, but not in the control cells treated with DMSO only (Figure S3). This lipid, as well as natural TMM and TDM from the same sample of ^{14}C -labeled lipids, was isolated by preparative TLC and incubated overnight with 15% tetrabutylammonium hydroxide (TBAH) at 100 °C to release

bound fatty and mycolic acids. Free fatty and mycolic acids were further derivatized to corresponding methyl esters and analyzed by TLC in *n*-hexane/ethyl acetate (95:5, 3 runs). These analyses revealed that the strongly fluorescent spot **16-A**, like TMM and TDM, carries all forms of mycolic acids (α , α' , and epoxy) typical for *M. smegmatis* (Figure 4C). Repetition of the experiment using *M. tuberculosis* H37Ra validated the same mechanism of action in both species (Figure S4). Moreover, the simultaneous treatment of *M. tuberculosis* H37Ra with compound **16** and isoniazid (INH) led to the disappearance not only of TMM and TDM, but also of the lipid **16-A**. Isoniazid inhibits enoyl-ACP-reductase that participates in the synthesis of mycolic acids,³³ thus confirming mycolic acid content of **16-A**. To show that the Ag85 complex is responsible for processing of the trehalose conjugates in mycobacteria, we pretreated cells of *M. smegmatis* with Ebselen, an experimental Ag85 complex inhibitor following the protocol published by Kamariza et al.⁸ Subsequently, cells were treated with **16** or **4**. After 6 h of incubation at 37 °C, cells were washed twice to remove nonspecifically bound probe, and incorporation was assessed by quantifying fluorescence of the attached BODIPY dye at 525/600 nm. Indeed, pretreatment leads to a 60% diminished incorporation of compound **16** in the presence of 100 μM Ebselen, in accordance to literature values⁸ (Figure 4D). This demonstrates the requirement of a functional Ag85 complex for probe integration. Additionally, we constructed a CRISPRi mutant, downregulating *lpqY* (observed suppression level of 50% under the applied conditions, Figure S5), an essential component of the trehalose reuptake ABC transporter³⁴ and found that incorporation of **16** does not primarily rely on the intracellular trehalose metabolism (Figures 1 and 4). This finding is consistent with the proposed synthesis of TDM occurring at the outer site of the plasma membrane and the localization of Ag85 complex enzymes in this space.

To further investigate the general applicability of the photosensitizer trehalose conjugates, we tested the most

promising derivatives also in *M. abscessus*.^{35,36} *M. abscessus* belongs to the group of nontuberculous mycobacteria and is a rapidly growing multi-drug-resistant *bacillus*, responsible for a wide spectrum of skin and soft tissue diseases but also pulmonary or central nervous system infections, mostly in immunocompromised individuals.³⁷ The incidence and prevalence of these infections have been increasing worldwide. Consequently, nontuberculous mycobacteria are also recognized as important human pathogens that contribute to an emerging public health problem.³⁸ Severe infections have been reported in association with acupuncture treatments, mesotherapy, or liposuction procedures caused by *M. abscessus* or *Mycobacterium chelonae* (*M. chelonae*). Considering that our conjugates need activation by light, they are potential candidates for the treatment of dermal lesions. Since the Ag85 complex is uniformly present in all mycobacterial species, we hypothesized that incorporation of these compounds in general is very likely and that they will be comparably potent in *M. abscessus*. MIC values of the tested compounds are summarized in Table 1. All tested compounds were nontoxic in the absence of light up to the highest concentration tested (200 μ M). Compounds 14 and 16 were potent in killing *M. abscessus* with an MIC value of 0.52 and 0.78 μ M, respectively, after light activation. The observed MICs are comparable with literature values from currently applied drugs in therapy such as amikacin, kanamycin, or apramycin (MIC = 3, 2, and 0.9 μ M, respectively).^{38,39} Furthermore, the values obtained for 14 as well as 16, and the respective nonconjugated photosensitizers 4 and 5, are in firm agreement with the observations made for *M. smegmatis*, indicating the same mechanism of action in both species. In contrast, 11 was significantly less active than 1 and also 10; we find that attachment of trehalose reduces the phototoxicity of PPIX (1) in the presence of light from 0.26 to 3.1 μ M (10) and 33 μ M (11), respectively. This finding points toward an intrinsic sensitivity of *M. abscessus* toward PPIX (1) after light irradiation, as compared to *M. smegmatis*, indicating a distinct mode of action in this species. Further studies are needed to investigate this interesting phenomenon. PPIX (1) is genuinely used in clinical settings as a photosensitizer, making this molecule an interesting candidate for further testing against clinical isolates of *M. abscessus*, as well as compounds 14 and 16, which were equally potent. Furthermore, we assessed cytotoxicity of our most active conjugates against mammalian cells (no photoactivation, see Figures S6 and S7) and found significantly high apparent IC₅₀ values of 28 \pm 3.9 μ M (16) and 61 \pm 6.6 μ M (14), opening a potential window for localized treatment of photosensitizer-enriched mycobacteria. Trehalose conjugation thus appears to be a highly promising strategy to increase both the activity and selectivity of photosensitizers.

CONCLUSION

We have demonstrated that phototoxic molecules such as 14 or 16 could be promising candidates for the targeted treatment of mycobacterial infections and for further development into sterilizing antimycobacterial agents. The unique mechanism is based on the recognition of these molecules by mycobacterial Ag85 complex catalyzing their esterification with mycolic acids. The incorporation of the resulting lipids into the mycomembrane and subsequent generation of singlet oxygen by irradiation renders the molecules less susceptible to potential detoxification via drug efflux pumps. Moreover, the mycobacterial inner membrane, which is a recognized permeation

barrier, does not need to be crossed by our conjugates, since Ag85 complex enzymes act at the outer side of the plasma membrane. In summary, our study indicates that trehalose conjugates of photosensitizers represent an exciting new class of antimycobacterial agents that warrant further development.

For methods, please refer to the Supporting Information.

ASSOCIATED CONTENT

Supporting Information

The Supporting Information is available free of charge on the ACS Publications website at DOI: 10.1021/acscentsci.8b00962.

Additional experimental details, data, and figures including NMR spectra and HPLC chromatograms (PDF)

AUTHOR INFORMATION

Corresponding Author

*E-mail: claudia.jessen-trefzer@pharmazie.uni-freiburg.de.

ORCID

Henning J. Jessen: 0000-0002-1025-9484

Claudia Jessen-Trefzer: 0000-0003-4216-8189

Author Contributions

A.D., J.K., M.Z., M.F., X.W., P.L., N.A., C.J.-T., and E.C. performed the experimental work. C.J.-T. designed the project. C.J.-T., J.K., A.D., and H.J.J. wrote the manuscript. The manuscript was finalized through contributions of all authors. All authors have given approval to the final version of the manuscript.

Notes

The authors declare no competing financial interest.

Safety statement: no unexpected or unusually high safety hazards were encountered.

ACKNOWLEDGMENTS

We thank Prof. Dr. William R. Jacobs Jr. for providing the strain *M. smegmatis* mc²15S, Mr. Sören Hammelmann and Mr. Stephan Munding for technical assistance during chemical synthesis, Dr. Katarína Mikušová for helpful discussions, and Judy Wong for proof-reading the manuscript. This work was supported by the Chinese Research Council (X.W.), the Ministry of Science, Research and the Arts Baden-Württemberg (C.J.-T., Grant 33-7533-30-10/25/27), the Department of Biotechnology, Govt. of India (N.A., Grants BT/PR19140/MED/29/1104/2016 and BT/PR8616/MED/29/793/2013), and the Ministry of Education, Science, Research and Sport of the Slovak Republic (J.K., Grant 0395/2016 for Slovak/Russian cooperation in science 2015-15075/33841:1-15E0 and grant VEGA 1/0301/18).

REFERENCES

- (1) Jarlier, V.; Nikaido, H. Mycobacterial cell wall: Structure and role in natural resistance to antibiotics. *FEMS Microbiol. Lett.* **1994**, *123*, 11–18.
- (2) Nguyen, L.; Thompson, C. J. Foundations of antibiotic resistance in bacterial physiology: the mycobacterial paradigm. *Trends Microbiol.* **2006**, *14* (7), 304–312.
- (3) Da Silva, P. E.; Von Groll, A.; Martin, A.; Palomino, J. C. Efflux as a mechanism for drug resistance in *Mycobacterium tuberculosis*. *FEMS Immunol. Med. Microbiol.* **2011**, *63* (1), 1–9.

- (4) Rodrigues, L.; Parish, T.; Balganes, M.; Ainsa, J. A. Antituberculosis drugs: reducing efflux = increasing activity. *Drug Discovery Today* **2017**, *22* (3), 592–599.
- (5) Li, X. Z.; Nikaido, H. Efflux-mediated drug resistance in bacteria: an update. *Drugs* **2009**, *69* (12), 1555–1623.
- (6) Backus, K. M.; Boshoff, H. L.; Barry, C. S.; Boutureira, O.; Patel, M. K.; D'Hooge, F.; Lee, S. S.; Via, L. E.; Tahlan, K.; Barry, C. E., 3rd; Davis, B. G. Uptake of unnatural trehalose analogs as a reporter for *Mycobacterium tuberculosis*. *Nat. Chem. Biol.* **2011**, *7* (4), 228–235.
- (7) Swarts, B. M.; Holsclaw, C. M.; Jewett, J. C.; Alber, M.; Fox, D. M.; Siegrist, M. S.; Leary, J. A.; Kalscheuer, R.; Bertozzi, C. R. Probing the mycobacterial trehalome with bioorthogonal chemistry. *J. Am. Chem. Soc.* **2012**, *134* (39), 16123–16126.
- (8) Kamariza, M.; Shieh, P.; Ealand, C. S.; Peters, J. S.; Chu, B.; Rodriguez-Rivera, F. P.; Babu Sait, M. R.; Treuren, W. V.; Martinson, N.; Kalscheuer, R.; Kana, B. D.; Bertozzi, C. R. Rapid detection of *Mycobacterium tuberculosis* in sputum with a solvatochromic trehalose probe. *Sci. Transl. Med.* **2018**, *10* (430), 1–12.
- (9) Foley, H. N.; Stewart, J. A.; Kavunja, H. W.; Rundell, S. R.; Swarts, B. M. Bioorthogonal chemical reporters for selective in situ probing of mycomembrane components in mycobacteria. *Angew. Chem., Int. Ed.* **2016**, *55* (6), 2053–2057.
- (10) Gavalda, S.; Bardou, F.; Laval, F.; Bon, C.; Malaga, W.; Chalut, C.; Guilhot, C.; Mourey, L.; Daffé, M.; Quémar, A. The polyketide synthase Pks13 catalyzes a novel mechanism of lipid transfer in mycobacteria. *Chem. Biol.* **2014**, *21* (12), 1660–1669.
- (11) Belisle, J. T.; Vissa, V. D.; Sievert, T.; Takayama, K.; Brennan, P. J.; Besra, G. S. Role of the major antigen of *Mycobacterium tuberculosis* in cell wall biogenesis. *Science* **1997**, *276* (5317), 1420–1422.
- (12) Jackson, M.; Raynaud, C.; Lanéelle, M. A.; Guilhot, C.; Laurent-Winter, C.; Ensergueix, D.; Gicquel, B.; Daffé, M. Inactivation of the antigen 85C gene profoundly affects the mycolate content and alters the permeability of the *Mycobacterium tuberculosis* cell envelope. *Mol. Microbiol.* **1999**, *31* (5), 1573–1587.
- (13) Armitage, L. Y.; Jagannath, C.; Wanger, A. R.; Norris, S. J. Disruption of the genes encoding antigen 85A and antigen 85B of *Mycobacterium tuberculosis* H37Rv: effect on growth in culture and in macrophages. *Infect. Immun.* **2000**, *68* (2), 767–778.
- (14) Viljoen, A.; Richard, M.; Nguyen, P. C.; Fourquet, P.; Camoin, L.; Paudal, R. R.; Gnawali, G. R.; Spilling, C. D.; Cavalier, J. F.; Canaan, S.; Blaise, M.; Kremer, L. Cyclopostins and cyclophostin analogs inhibit the antigen 85C from. *J. Biol. Chem.* **2018**, *293* (8), 2755–2769.
- (15) Goins, C. M.; Dajnowicz, S.; Thanna, S.; Suchek, S. J.; Parks, J. M.; Ronning, D. R. Exploring covalent allosteric inhibition of antigen 85C from *Mycobacterium tuberculosis* by ebsele derivatives. *ACS Infect. Dis.* **2017**, *3* (5), 378–387.
- (16) Lehmann, J.; Cheng, T. Y.; Aggarwal, A.; Park, A. S.; Zeiler, E.; Raju, R. M.; Akopian, T.; Kandror, O.; Sacchettini, J. C.; Moody, D. B.; Rubin, E. J.; Sieber, S. A. An antibacterial β -Lactone kills *Mycobacterium tuberculosis* by disrupting mycolic acid biosynthesis. *Angew. Chem., Int. Ed.* **2018**, *57* (1), 348–353.
- (17) Nguyen, P. C.; Delorme, V.; Bénarouche, A.; Martin, B. P.; Paudel, R.; Gnawali, G. R.; Madani, A.; Puppo, R.; Landry, V.; Kremer, L.; Brodin, P.; Spilling, C. D.; Cavalier, J. F.; Canaan, S. Cyclopostins and Cyclophostin analogs as promising compounds in the fight against tuberculosis. *Sci. Rep.* **2017**, *7* (1), 11751.
- (18) Favrot, L.; Grzegorzewicz, A. E.; Lajiness, D. H.; Marvin, R. K.; Boucau, J.; Isailovic, D.; Jackson, M.; Ronning, D. R. Mechanism of inhibition of *Mycobacterium tuberculosis* antigen 85 by ebsele. *Nat. Commun.* **2013**, *4*, 2748.
- (19) Kamkaew, A.; Lim, S. H.; Lee, H. B.; Kiew, L. V.; Chung, L. Y.; Burgess, K. BODIPY dyes in photodynamic therapy. *Chem. Soc. Rev.* **2013**, *42* (1), 77–88.
- (20) Chang, J. E.; Oak, C. H.; Sung, N.; Jheon, S. The potential application of photodynamic therapy in drug-resistant tuberculosis. *J. Photochem. Photobiol., B* **2015**, *150*, 60–65.
- (21) O'Riordan, K.; Sharlin, D. S.; Gross, J.; Chang, S.; Errabelli, D.; Akilov, O. E.; Kosaka, S.; Nau, G. J.; Hasan, T. Photoinactivation of *Mycobacteria* in vitro and in a new murine model of localized *Mycobacterium bovis* BCG-induced granulomatous infection. *Antimicrob. Agents Chemother.* **2006**, *50* (5), 1828–1834.
- (22) Feese, E.; Ghiladi, R. A. Highly efficient in vitro photodynamic inactivation of *Mycobacterium smegmatis*. *J. Antimicrob. Chemother.* **2009**, *64* (4), 782–785.
- (23) Kou, J.; Dou, D.; Yang, L. Porphyrin photosensitizers in photodynamic therapy and its applications. *Oncotarget* **2017**, *8* (46), 81591–81603.
- (24) Lim, S. H.; Thivierge, C.; Nowak-Sliwinska, P.; Han, J.; van den Bergh, H.; Wagnières, G.; Burgess, K.; Lee, H. B. In vitro and in vivo photocytotoxicity of boron dipyrromethene derivatives for photodynamic therapy. *J. Med. Chem.* **2010**, *53* (7), 2865–2874.
- (25) Chen, Y.; Zhao, J.; Xie, L.; Guo, H.; Li, Q. Thienyl-substituted BODIPYs with strong visible light-absorption and long-lived triplet excited states as organic triplet sensitizers for triplet–triplet annihilation upconversion. *RSC Adv.* **2012**, *2*, 3942–3953.
- (26) Tardivo, J. P.; Del Giglio, A.; de Oliveira, C. S.; Gabrielli, D. S.; Junqueira, H. C.; Tada, D. B.; Severino, D.; de Fatima Turchiello, R.; Baptista, M. S. Methylene blue in photodynamic therapy: From basic mechanisms to clinical applications. *Photodiagn. Photodyn. Ther.* **2005**, *2* (3), 175–191.
- (27) Hanessian, S.; Lavalée, P. Synthesis of 6-amino-6-deoxy-, -trehalose: a positional isomer of trehalosamine. *J. Antibiot.* **1972**, *25* (11), 683–684.
- (28) de Groot, J. J.; van Vliet, J. A. J. M.; Waszink, J. H. The high pressure sodium lamp. *Philips Tech Rev.* **1975**, *35* (11–12), 334–342.
- (29) Grzegorzewicz, A. E.; Pham, H.; Gundi, V. A.; Scherman, M. S.; North, E. J.; Hess, T.; Jones, V.; Gruppo, V.; Born, S. E.; Korduláková, J.; Chavadi, S. S.; Morisseau, C.; Lenaerts, A. J.; Lee, R. E.; McNeil, M. R.; Jackson, M. Inhibition of mycolic acid transport across the *Mycobacterium tuberculosis* plasma membrane. *Nat. Chem. Biol.* **2012**, *8* (4), 334–341.
- (30) Pal, R.; Ansari, M. A.; Saibabu, V.; Das, S.; Fatima, Z.; Hameed, S. Nonphotodynamic roles of methylene blue: display of distinct antimycobacterial and anticandidal mode of actions. *J. Pathog.* **2018**, *2018*, 3759704.
- (31) Kim, S.; Fujitsuka, M.; Majima, T. Photochemistry of singlet oxygen sensor green. *J. Phys. Chem. B* **2013**, *117* (45), 13985–13992.
- (32) Folch, J.; Lees, M.; Sloane Stanley, G. H. A simple method for the isolation and purification of total lipides from animal tissues. *J. Biol. Chem.* **1957**, *226* (1), 497–509.
- (33) Banerjee, A.; Dubnau, E.; Quemard, A.; Balasubramanian, V.; Um, K. S.; Wilson, T.; Collins, D.; de Lisle, G.; Jacobs, W. R., Jr. inhA, a gene encoding a target for isoniazid and ethionamide in *Mycobacterium tuberculosis*. *Science* **1994**, *263* (5144), 227–230.
- (34) Kalscheuer, R.; Weinrick, B.; Veeraghavan, U.; Besra, G. S.; Jacobs, W. R. Trehalose-recycling ABC transporter LpqY-SugA-SugB-SugC is essential for virulence of *Mycobacterium tuberculosis*. *Proc. Natl. Acad. Sci. U. S. A.* **2010**, *107* (50), 21761–21766.
- (35) Elston, D. Nontuberculous mycobacterial skin infections: recognition and management. *Am. J. Clin. Dermatol.* **2009**, *10* (5), 281–285.
- (36) De Groote, M. A.; Huitt, G. Infections due to rapidly growing mycobacteria. *Clin. Infect. Dis.* **2006**, *42* (12), 1756–1763.
- (37) Lee, M. R.; Sheng, W. H.; Hung, C. C.; Yu, C. J.; Lee, L. N.; Hsueh, P. R. *Mycobacterium abscessus* complex infections in humans. *Emerging Infect. Dis.* **2015**, *21* (9), 1638–1646.
- (38) Luthra, S.; Rominski, A.; Sander, P. The role of antibiotic-target-modifying and antibiotic-modifying enzymes in *Mycobacterium abscessus* drug resistance. *Front. Microbiol.* **2018**, *9*, 2179.
- (39) Rominski, A.; Selchow, P.; Becker, K.; Brulle, J. K.; Dal Molin, M.; Sander, P. Elucidation of *Mycobacterium abscessus* aminoglycoside and capreomycin resistance by targeted deletion of three putative resistance genes. *J. Antimicrob. Chemother.* **2017**, *72* (8), 2191–2200.